Contents list available at CBIORE journal website

International Journal of Renewable Energy Development

Journal homepage: https://ijred.cbiore.id

Research Article

Statistical optimization of acid hydrolysis of *Eichhornia crassipes* for soluble sugar recovery based on physicochemical interpretation of process interactions

Daniel Montalvo*[a], Benjamín Álvarez-Alor[a], Jesús Alonso Cruz-Valdez[a], Israel Isaac Zetina-Rios[a], Pedro-Eusebio Alvarado-Méndez[a], José Manuel Pérez-Francisco[a], Ruby Sheila Gines-Palestino[b]

[a]*Tecnológico Nacional de México/Instituto Tecnológico Superior de Coatzacoalcos, Carretera Antigua Minatitlán-Coatzacoalcos km 16.5, Coatzacoalcos, Veracruz, 96535, México.*

[b]*Facultad de Ciencias Químicas, Universidad Veracruzana, Prolongación Oriente 6 No. 1009, Col. Rafael Alvarado, Orizaba, C.P. 94340, Veracruz, México*

Abstract. Aquatic invasive plants are an underused source of renewable biomass, particularly when their uncontrolled proliferation creates environmental management challenges. The lignocellulosic fractions may provide fermentable-sugar precursors without competing directly with conventional food-crop production systems. However, efficiently converting lignocellulosic biomass into fermentable sugars remains one of the main challenges for sustainable biorefineries. This study tested the hypothesis that dilute-acid hydrolysis of *Eichhornia crassipes* can be optimized to maximize fermentable sugar release while elucidating the physicochemical mechanisms governing the process. A Box–Behnken response surface design was employed to evaluate the effects of temperature (110–130 °C), sulfuric acid concentration (1–3%), and solid-to-liquid ratio (1:5–1:9) on total sugar production. Statistical analyses demonstrated that temperature was the dominant factor controlling hydrolysis, whereas acid concentration and solid-to-liquid ratio regulated catalytic selectivity and mass-transfer limitations. The quadratic model adequately described the experimental response (R^2 = 0.81), and its mechanistic interpretation revealed that sugar production results from the competition between polysaccharide depolymerization and monosaccharide degradation. Experimental validation confirmed the robustness of the optimized conditions, with an average prediction error of 15% and a mean sugar concentration of 79.5 ± 6.31 g·L^{-1}. Mass balance analysis showed an average recovery of 0.636 g of soluble sugars, corresponding to 47.1% of the theoretical structural carbohydrate potential. These findings provide a quantitative basis for understanding and optimizing the acid hydrolysis of *Eichhornia crassipes*. The results also support the potential use of this aquatic biomass as a renewable feedstock for future biorefinery applications.

Keywords: Lignocellulosic biomass, biomass valorization, water hyacinth structural carbohydrates, Box–Behnken design.

@ The author(s). Published by CBIORE. This is an open access article under the CC BY-SA license (https://creativecommons.org/licenses/by-sa/4.0/).

Received: 30th July 2026; Revised: 19th Oct 2026; Accepted: 2nd Nov 2026; Available online: 7th Nov 2026

1. Introduction

The transition toward a circular economy has accelerated the search for renewable feedstocks to replace fossil resources in the production of fuels and biobased chemicals. Within this framework, lignocellulosic biomass has emerged as one of the most promising raw materials because it is abundant, renewable, and does not compete directly with food production. Unlike first-generation bioethanol, which relies on edible crops such as corn and sugarcane, second-generation bioethanol uses structural carbohydrates from agricultural residues, forestry wastes, and non-food biomass, offering significant environmental and economic advantages by promoting waste valorization and reducing greenhouse gas emissions. Consequently, the efficient conversion of lignocellulosic biomass into fermentable sugars has become a key step in the development of sustainable biorefineries (Ashokkumar *et al.*, 2022; Velvizhi *et al.*, 2022).

Among lignocellulosic feedstocks, aquatic biomass has attracted increasing attention due to its rapid growth and the environmental problems associated with its uncontrolled proliferation. *Eichhornia crassipes* (*E. crassipes*, water hyacinth), a floating perennial monocot native to the Amazon basin, is considered one of the world's most aggressive invasive aquatic plants (Basaula *et al.*, 2023; Godana et al., 2022). Since its introduction outside South America during the nineteenth century as an ornamental species, it has spread rapidly throughout tropical and subtropical regions, colonizing lakes, rivers, irrigation canals, and reservoirs (Djihouessi *et al.*, 2023). Its extraordinary propagation rate results in dense floating mats that reduce light penetration, decrease dissolved oxygen concentrations, alter aquatic biodiversity, and severely affect freshwater ecosystem functioning. Beyond its ecological

* Corresponding author
Email: dmontalvos@itesco.edu.mx (D. Montalvo)

https://doi.org/10.61435/ijred.2027.63157
ISSN: 2252-4940(p)/ 2716-4519 (e)/© 2027.The Author(s). Published by CBIORE

impacts, water hyacinth imposes substantial socioeconomic costs by obstructing navigation, irrigation systems, hydroelectric facilities, fisheries, livestock watering, and water transportation, while increasing flood risks and the costs associated with mechanical removal and biomass disposal (Adeyeni *et al*., 2022; Damtie *et al*., 2021; Ingabire *et al*., 2023).

Despite being recognized primarily as an environmental nuisance (Udume *et al*., 2022), water hyacinth possesses characteristics that make it an attractive feedstock for biochemical conversion. Its cell wall is composed mainly of cellulose and hemicellulose with a relatively low lignin content compared with many terrestrial lignocellulosic biomasses, making the structural carbohydrates more accessible to chemical pretreatments (Rezania *et al*., 2017). Consequently, the biomass can be efficiently converted into soluble sugars that serve as precursors for producing bioethanol and other biobased products, such as ceramics (Babisk *et al*., 2023), hydrogels (Elma *et al*., 2023) . Recent studies have reported high sugar yields and hemicellulose conversion efficiencies after optimized pretreatment, highlighting the considerable potential of *E. crassipes* within integrated biorefinery schemes (Ding *et al*., 2024; Romero-Borbón *et al*., 2022). Therefore, the environmental burden associated with this invasive species can be transformed into an opportunity for biomass valorization, simultaneously contributing to aquatic ecosystem restoration and renewable energy production.

Among the available pretreatment technologies, dilute-acid hydrolysis remains one of the most effective approaches for releasing fermentable sugars from lignocellulosic biomass because it selectively hydrolyzes hemicellulose and increases cellulose accessibility by disrupting the structural organization of the plant cell wall. The efficiency of this process is strongly influenced by operating variables such as temperature, acid concentration, and solid-to-liquid ratio, which simultaneously govern proton diffusion, cleavage of glycosidic bonds, sugar solubilization, and the formation of degradation products including furfural and 5-hydroxymethylfurfural (HMF). Consequently, the severity of hydrolysis must be carefully controlled to maximize sugar production while minimizing secondary degradation reactions (Atilago *et al*., 2025; Chinwatpaiboon *et al*., 2023; Q. Zhang *et al*., 2018).

Although considerable progress has been made in developing pretreatment technologies and integrating water hyacinth into biorefinery schemes, most studies have focused primarily on maximizing sugar or biofuel yields through process optimization. Recent reviews emphasize that future research should move beyond yield-oriented approaches by integrating mechanistic understanding, experimental validation, mass balance analysis, and process scalability to establish technically reliable conversion routes for industrial implementation. Likewise, integrated biorefineries capable of simultaneously producing bioethanol, biogas, biohydrogen, and other value-added products have been identified as a key research direction to improve resource efficiency and support circular bioeconomy strategies (Phan *et al*., 2025). Nevertheless, the physicochemical mechanisms governing dilute-acid hydrolysis, the mechanistic interpretation of statistical optimization models, and the quantitative evaluation of structural carbohydrate recovery remain poorly understood for Eichhornia crassipes. Addressing these knowledge gaps is essential for developing predictive and transferable hydrolysis processes suitable for second-generation biorefineries (Abba *et al*., 2025; Bajpai & Nemade, 2023).

Based on these considerations, the present study was guided by the hypothesis that dilute sulfuric acid hydrolysis of *E. crassipes* can be optimized to maximize the release of fermentable sugars and that the physicochemical mechanisms controlling sugar production can be elucidated through statistical modeling combined with mechanistic interpretation. Therefore, the objective of this work was to optimize the dilute-acid hydrolysis of *E. crassipes* using a Box–Behnken design (BBD) by evaluating the effects of temperature, sulfuric acid concentration, and solid-to-liquid ratio (RSL) on fermentable sugar production and to establish a robust basis for the subsequent production of second-generation bioethanol from this invasive aquatic biomass.

2. Materials and methods

2.1 Biomass collection and pretreatment

Water hyacinth (*E. crassipes*) biomass was collected from the Coatzacoalcos River, located in the city and port of Coatzacoalcos, Veracruz, México. The harvested biomass was first subjected to a size-reduction process to obtain particles of approximately 4 cm in length. Subsequently, the material was dried in a convection oven at 90 °C for 7 h to remove excess moisture from the leaves and stems. After drying, the biomass underwent a second size-reduction step to achieve a particle size of approximately 0.5 cm, thereby improving surface area and homogeneity for subsequent treatments. The dried and milled biomass was then subjected to a thermochemical pretreatment via acid hydrolysis to obtain fermentable sugars. For this purpose, 2 g of dry biomass were treated with sulfuric acid solution and processed in an autoclave at 15 psig for 25 min.

2.2 Experimental design for acid hydrolysis

To optimize fermentable sugar production via acid hydrolysis, a BBD was employed to evaluate the effects of key process variables. Three independent factors were considered: sulfuric acid concentration (1%, 2%, and 3% w/v), reaction temperature (110 °C, 120 °C, and 130 °C), and RSL (1:5, 1:7, and 1:9). The response variable was the concentration of reducing sugars obtained after hydrolysis. A total of 60 independent experiments were carried out, comprising an experimental design matrix with three replicates per treatment to ensure statistical reliability and reduce experimental error. This approach enabled the evaluation of individual and interactive effects of the variables, as well as the identification of optimal conditions to maximize sugar yield. Table 1 presents the design matrix with the natural variables evaluated.

Table 1
Design matrix of Box-Behnken design

Run	Temperature [°C]	Acid [%]	RSL
1	120	1	9
2	120	2	7
3	110	2	5
4	130	1	7
5	110	3	7
6	120	2	7
7	130	2	5
8	120	2	7
9	130	2	9
10	110	1	7
11	120	3	5
12	120	3	9
13	130	3	7
14	120	1	5
15	110	2	9

2.3 Total sugar determination and quantification

The total sugar concentration (TSc) in the hydrolysate was determined using the phenol-sulfuric acid method described by Dubois et al (Dubois *et al*., 1956). Briefly, 1 mL of the liquid fraction obtained after acid hydrolysis was collected and appropriately diluted. Subsequently, 1 mL of the sample was mixed with 2 mL of a 5% (w/v) phenol solution, followed by the rapid addition of 4 mL of concentrated sulfuric acid (98%). The mixture was allowed to react under ambient conditions to develop the characteristic color. The absorbance of the resulting solution was measured at 490 nm using a UV-Vis spectrophotometer. The TSc was quantified based on a calibration curve prepared with glucose as the standard. All measurements were performed in quadruplicate to ensure analytical reproducibility. This colorimetric method does not provide the selective identification or separate quantification of individual monosaccharides, such as glucose and xylose, nor does it allow the specific determination of degradation inhibitors such as furfural and 5-hydroxymethylfurfural (HMF). Therefore, the measured response is interpreted as total carbohydrate concentration.

2.4 Statistical analysis

The TSc data from the BBD were analyzed in Minitab 21.2 to assess the significance of the variables. The experimental data obtained from the BBD were fitted to a second-order polynomial model in order to describe the relationship between the independent variables and the response. The quadratic model is expressed as:

$$y = \beta_0 + \sum_{i=1}^{k} \beta_i x_i + \sum_{i=1}^{k} \beta_{ii} x_{ii}^2 + \sum_{i<j} \beta_{ij} x_i x_j \quad (1)$$

where y represents the response (TSc), β_0 is the intercept term, β_i are the linear coefficients, β_{ii} are the quadratic coefficients, β_{ij} are the interaction coefficients, and x_i is the coded factor level. The model's adequacy and the significance of each term were evaluated through analysis of variance (ANOVA). Statistical significance was determined at the 95% confidence level ($p < 0.05$). The quality of the fitted model was assessed using the coefficient of determination (R^2). The predictive capability of the quadratic model obtained from the BBD was experimentally validated under the optimum hydrolysis conditions predicted by the response surface analysis. Eight independent validation experiments were conducted using the optimized values for temperature, sulfuric acid concentration, and RSL. The hydrolysis procedure was performed following the same experimental protocol used during model development to ensure methodological consistency. Model performance was evaluated by calculating the relative prediction error according to Equation 2:

$$Prediction\ error\ (\%) = \frac{y_{exp} - y_{pred}}{y_{pred}} \times 100 \quad (2)$$

2.5 Mass balance and sugar recovery

A simplified mass balance was performed to quantify soluble sugar recovery under the optimum dilute-acid hydrolysis conditions. The analysis was based on eight validation experiments conducted with 2 g of dry *E. crassipes* biomass. The structural carbohydrate composition was estimated using literature-derived reference values of 31% cellulose and 29% hemicellulose (dry basis). These values were not experimentally determined for the specific biomass batch collected from the Coatzacoalcos River and were therefore used only as reference values for estimating the theoretical structural carbohydrate-derived sugar potential. Because the chemical composition of *E. crassipes* may vary according to geographical origin, plant fraction, growth conditions, and season (Mishima *et al*., 2008; Sierra *et al*., 2024; Tovar-Jiménez *et al*., 2019; Tucker & Debusk, 1981), the use of literature-derived composition values introduces uncertainty into the estimated theoretical sugar potential. The amount of soluble sugars recovered in each validation experiment was calculated from the total sugar concentration determined by the phenol–sulfuric acid method and the final volume of hydrolysate recovered after filtration according to Equation (3):

$$Recovered\ sugars\ (g) = S \times V \quad (3)$$

where S is the TSc ($g \cdot L^{-1}$), and V is the recovered hydrolysate volume (L). The theoretical structural carbohydrate-derived sugar potential was estimated using stoichiometric conversion factors based on the molecular weight ratio between the anhydro-sugar units present in the polysaccharides and their corresponding monomeric sugars. The repeating anhydroglucose unit in cellulose ($C_6H_{10}O_5$, 162.14 $g \cdot mol^{-1}$) yields one glucose molecule ($C_6H_{12}O_6$, 180.16 $g \cdot mol^{-1}$) after hydrolysis, resulting in a conversion factor of 1.111. Similarly, the anhydroxylose unit in xylan ($C_5H_8O_4$, 132.11 $g \cdot mol^{-1}$) produces one xylose molecule ($C_5H_{10}O_5$, 150.13 $g \cdot mol^{-1}$), corresponding to a conversion factor of 1.136. These stoichiometric factors were used to estimate the theoretical sugar potential of the biomass according to Equation (4):

$$Theoretical\ sugars(g) = (C \times 1.111) + (HC \times 1.136) \quad (4)$$

where C is the cellulose content, and HC is the hemicellulose content. Finally, sugar recovery was expressed as the percentage of experimentally recovered soluble sugars relative to the literature-derived theoretical structural carbohydrate potential according to Equation (5):

$$Sugar\ recovery\ (\%) = \frac{Recovered\ sugars\ (g)}{Theorical\ sugars\ (g)} \times 100 \quad (5)$$

3. Results and Discussion

Figure 1 presents the coefficient of variation (CV) for each treatment of the BBD. The CV is a relative measure of experimental dispersion that evaluates the reproducibility of the analytical procedure independently of the response magnitude. In response surface methodology (RSM), low experimental variability is essential for developing reliable predictive models

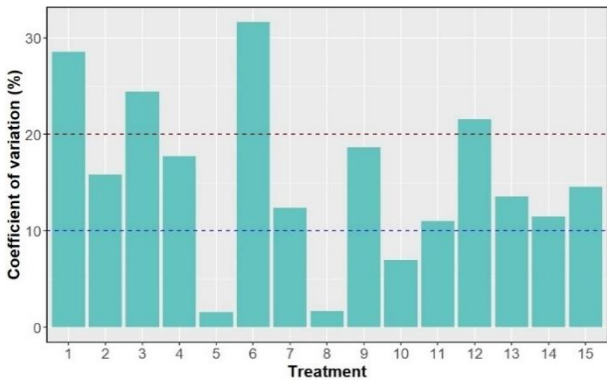


Fig. 1 Coefficient of variation of sugar yield for each experimental treatment in the BBD

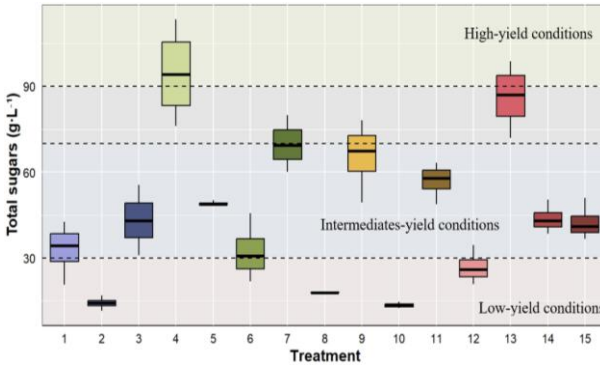


Fig. 3 Distribution of total sugar yield in the acid hydrolysis of water hyacinth under BBD

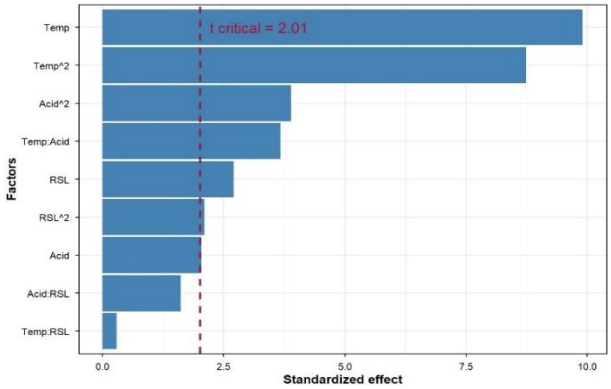


Fig. 2 Pareto chart of the standardized effects of process variables on sugar release during dilute-acid hydrolysis of *E. crassipes*

because experimental uncertainty is directly propagated into the estimation of the quadratic regression coefficients (Aragaw *et al*., 2025; Das *et al*., 2015). The CV values ranged from 1.5 to 31.6%, indicating that the experimental precision depended on the hydrolysis conditions. Most treatments exhibited CV values below 20%, while several were below 10%, demonstrating satisfactory repeatability of the phenol–sulfuric acid method. Therefore, the overall variability is mainly associated with the hydrolysis process rather than with the analytical quantification.

Higher dispersion was observed for Treatments 1, 3, 6, and 12, which can be attributed to the intrinsic heterogeneity of *E. crassipes*. Variations in cellulose, hemicellulose, lignin, extractives, and ash among plant tissues influence acid penetration and the accessibility of structural polysaccharides, resulting in different hydrolysis rates and sugar yields (Singh *et al*., 2020). Notably, the highest CV values were associated with intermediate hydrolysis severity, where partial depolymerization of hemicellulose makes the process particularly sensitive to small structural differences in the biomass. Under more severe conditions, polysaccharide solubilization becomes more uniform; however, excessive severity can promote the simultaneous degradation of released monosaccharides into secondary products, increasing the response variability. Thus, the observed dispersion is attributed to the competitive kinetics between polysaccharide hydrolysis and sugar degradation.

Figure 2 illustrates the distribution of sugar yields obtained from the acid hydrolysis of *E. crassipes* under the BBD. TSc ranged from approximately 13 to 113 $g{\cdot}L^{-1}$, revealing a broad experimental response and confirming that the selected operating conditions generated markedly different hydrolysis efficiencies. The boxplots show three distinct response regions: (i) low sugar yields or limited hydrolysis (<30 $g{\cdot}L^{-1}$), (ii) intermediate yields or transition (maximum sensitivity to operating conditions) (40–70 $g{\cdot}L^{-1}$), and (iii) high-yield conditions or efficient hydrolysis (>90 $g{\cdot}L^{-1}$). This wide distribution demonstrates that the hydrolysis process is highly sensitive to operating conditions and provides sufficient experimental variability to develop a predictive response surface model.

The observed response distribution reflects the sequential nature of lignocellulosic hydrolysis. Under mild conditions, proton diffusion into the lignocellulosic matrix is limited, restricting the cleavage of β-(1→4)-glycosidic bonds within the hemicellulose fraction and consequently reducing the release of soluble sugars. As hydrolysis severity increases, disruption of the plant cell wall enhances polysaccharide accessibility and promotes sugar liberation. However, excessive reaction severity can dehydrate released monosaccharides to secondary products such as furfural and 5-hydroxymethylfurfural (HMF), thereby reducing the net concentration of total sugars (Deng *et al*., 2023; Zhou *et al*., 2021).

Another relevant feature revealed by the boxplots is the variability observed among treatments. While several experimental conditions exhibited narrow interquartile ranges, indicating stable sugar production, others showed broader distributions, suggesting that sugar release was highly sensitive to small variations in biomass composition or reaction conditions. Such behavior is commonly reported for lignocellulosic feedstocks because differences in cellulose, hemicellulose, lignin, and extractive contents influence acid accessibility and hydrolysis kinetics (Singh *et al*., 2020). These observations support the need for a multivariate optimization strategy that can simultaneously evaluate the effects and interactions of the operating variables.

Figure 3 presents the Pareto chart of the standardized effects. The analysis reveals that temperature was the dominant factor controlling the process, followed by its quadratic term ($Temp^2$), the quadratic effect of acid concentration ($Acid^2$), the temperature × acid interaction, and the linear effect of the RSL. This hierarchy indicates that sugar release is primarily governed by the severity of hydrolysis rather than by the independent contribution of each operating variable.

The temperature effect indicates that temperature controls both the cleavage of glycosidic bonds and the structural accessibility of the substrate, serving as the main driver of the conversion of polysaccharides into fermentable sugars (Deng *et al*., 2023), while quadratic effects of temperature demonstrate that thermal severity simultaneously promotes biomass deconstruction and sugar degradation. Increasing temperature enhances proton diffusion into the lignocellulosic matrix, accelerates cleavage of β-(1→4)-glycosidic bonds in hemicellulose, and weakens the hydrogen-bonding network that limits cellulose accessibility. However, the significance of the $Temp^2$ term indicates that this effect is nonlinear. Beyond an optimum severity, dehydration reactions become dominant, converting sugars such as pentoses and hexoses into furfural and HMF, thereby reducing the net concentration of total sugars. This transition from sugar formation to sugar degradation has been recognized as the principal kinetic feature of dilute-acid pretreatment of lignocellulosic biomass (Du Pasquier *et al*., 2023; Zhou *et al*., 2021). This behavior has been widely described as characteristic of acid-catalyzed systems; under non-mild conditions (high temperatures), the process's selectivity is reduced (McNamara *et al*., 2024).

The significance of $Acid^2$, despite the linear acid effect remaining statistically insignificant, indicates that proton concentration primarily controls hydrolysis selectivity rather

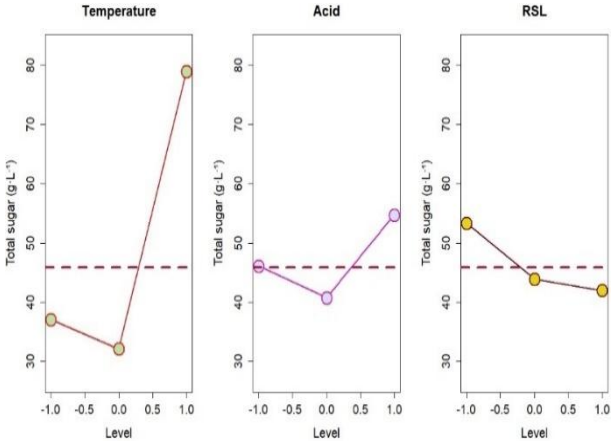


Fig. 5 Main effects of temperature, acid concentration, and RSL on total sugar production during dilute-acid hydrolysis of *E. crassipes*

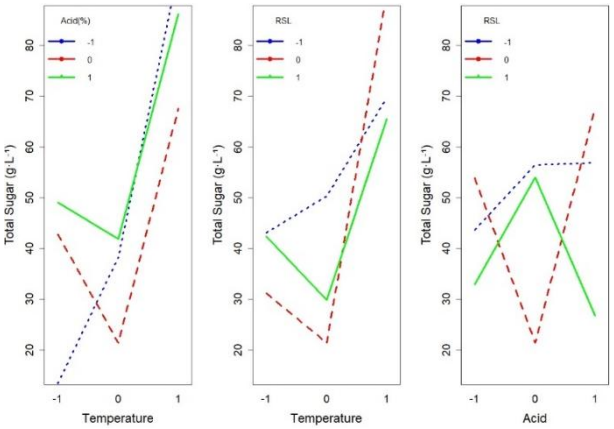


Fig. 4 Interaction effects of temperature, acid concentration, and RSL on total sugar production during dilute-acid hydrolysis of *E. crassipes*

than reaction rate. At low acid concentrations, the availability of protons is insufficient to efficiently protonate glycosidic oxygen atoms, thereby limiting polysaccharide depolymerization. Conversely, excessive proton activity accelerates dehydration and condensation reactions, reducing fermentable sugar recovery. Therefore, acid concentration exhibits an optimum operating window in which hydrolysis predominates over degradation (Yuan *et al.*, 2021; Zhou *et al.*, 2021).

The significant temperature × acid interaction further demonstrates that both variables act synergistically. Acid catalysis becomes increasingly effective as temperature enhances molecular mobility and acid diffusion through the plant cell wall, whereas higher temperatures also amplify acid-catalyzed degradation reactions. Consequently, neither variable can be interpreted independently because the final sugar yield results from the balance between catalytic hydrolysis and secondary degradation pathways. Similar synergistic effects have been reported during dilute-acid pretreatment of herbaceous lignocellulosic biomass (Du Pasquier *et al.*, 2023).

Although the linear effect of RSL was less pronounced than temperature-related effects, its statistical significance highlights the importance of mass-transfer phenomena. Adequate liquid availability facilitates acid penetration into the lignocellulosic structure and promotes diffusion of soluble hydrolysis products, whereas excessive solids loading generates concentration gradients that limit reagent accessibility and reduce hydrolysis efficiency. Thus, sugar production is governed by the combined influence of reaction kinetics, catalytic proton activity, and transport phenomena within the biomass matrix (Lv *et al.*, 2024; Sun *et al.*, 2023).

Figure 4 displays the main effects of the operating variables on total sugar production during the dilute-acid hydrolysis of *E. crassipes*. Consistent with the Pareto analysis, temperature had the greatest effect on the response, with sugar concentration increasing markedly from low to high levels. This behavior confirms that thermal severity is the primary driving force for lignocellulosic deconstruction, as higher temperatures enhance proton diffusion into the biomass matrix, accelerate cleavage of β-(1→4)-glycosidic bonds in hemicellulose, and partially disrupt the hydrogen-bonding network that limits cellulose accessibility. Consequently, the accessibility of structural polysaccharides increases, promoting the release of soluble fermentable sugars (Du Pasquier *et al.*, 2023; Zhou *et al.*, 2021).

In contrast, the acid concentration showed a minimal response at intermediate levels, with lower sugar yields than at the highest concentration. This trend suggests that acid concentration primarily regulates hydrolysis selectivity by balancing cleavage of the glycosidic bond with the initiation of secondary dehydration reactions. Under dilute acid conditions, proton availability controls the catalytic depolymerization of hemicellulose, while excessive reaction severity simultaneously promotes the conversion of the released monosaccharides to furfural and HMF. Therefore, the acid concentration response cannot be interpreted independently of thermal conditions, anticipating the interaction effects assessed in the subsequent analysis (Świątek *et al.*, 2020; Yuan *et al.*, 2021).

The RSL showed a moderate negative trend, indicating that the increased solids loading reduced the overall sugar recovery. This behavior is primarily associated with mass-transfer limitations rather than intrinsic reaction kinetics. At higher solids concentrations, acid diffusion within the lignocellulosic structure becomes less efficient, local proton concentration gradients develop, and the removal of hydrolysis products is hindered, thus reducing the catalytic accessibility to the structural carbohydrates. The observed reduction in catalytic efficiency at higher solid loadings is consistent with previous studies on the dilute-acid hydrolysis of lignocellulosic biomass, where hydrolysis efficiency is governed by the combined effects of reaction kinetics and mass-transfer phenomena, whereas temperature and acid concentration regulate hydrolysis severity and the selectivity toward sugar production (Świątek *et al.*, 2020; B. Zhang *et al.*, 2022; J. Zhang *et al.*, 2020).

Figure 5 illustrates the interaction effects among the operating variables, demonstrating that fermentable sugar production depends on the combined influence of reaction severity rather than on the independent contribution of each factor. The non-parallel profiles observed across all interaction plots indicate that the effect of one variable varies with the level of the second variable, confirming that dilute-acid hydrolysis is governed by coupled kinetic and transport phenomena.

The temperature×acid interaction exhibited the strongest dependence, corroborating the significance observed in the Pareto analysis. At elevated temperatures, increasing acid concentration substantially enhanced sugar release because higher thermal energy accelerates proton diffusion into the lignocellulosic matrix and promotes proton-catalyzed cleavage of β-(1→4)-glycosidic bonds in hemicellulose. However, the steep response at the highest severity also suggests the onset of competitive dehydration reactions, in which liberated pentoses and hexoses are converted into furfural and HMF (Delbecq *et al.*, 2018). Therefore, temperature and acid concentration act synergistically by increasing hydrolysis efficiency, but excessive severity progressively reduces process selectivity through sugar degradation (Du Pasquier *et al.*, 2023; Zhou *et al.*, 2021).

The temperature×RSL interaction indicates that thermal effects are strongly influenced by mass-transfer conditions. At low solid loading, acid penetration and diffusion of soluble hydrolysis products are favored, allowing temperature to efficiently promote biomass deconstruction. Conversely, increasing the solid fraction limits acid accessibility to the plant cell wall, generating diffusional resistance that reduces the effectiveness of thermal activation. These results demonstrate that hydrolysis efficiency is governed by both intrinsic reaction kinetics and internal transport phenomena within the lignocellulosic matrix (Lv *et al*., 2024; Sun *et al*., 2023).

The acid×RSL interaction exhibited a less pronounced but still relevant effect, suggesting that proton availability and liquid accessibility jointly regulate catalytic efficiency. Higher acid concentrations cannot fully compensate for insufficient liquid availability because restricted diffusion limits proton transport to reactive sites within the biomass. Consequently, the catalytic potential of sulfuric acid depends not only on its concentration but also on its effective distribution throughout the lignocellulosic structure. Similar coupling between catalyst accessibility and biomass porosity has been reported during dilute-acid pretreatment of herbaceous feedstocks (Du Pasquier *et al*., 2023).

Figure 6 shows the quadratic response model (Equation 6, R^2 = 0.81) and displays the operating region that maximizes sugar production through the simultaneous interaction of temperature, sulfuric acid concentration, and RSL. The response surfaces reveal that TSc is controlled by a narrow optimum region generated by the balance between polysaccharide depolymerization, catalyst accessibility, and secondary sugar degradation. The continuous curvature observed in the three surfaces confirms the nonlinear nature of dilute-acid hydrolysis, where increasing process severity does not necessarily result in proportional increases in sugar yield.

The temperature-acid surface (Figure 6a) exhibits the steepest response gradient, indicating that both variables jointly determine hydrolysis severity. Increasing temperature accelerates proton diffusion and enhances cleavage of β-(1→4)-glycosidic bonds within hemicellulose while simultaneously reducing the structural resistance imposed by hydrogen-bonded cellulose microfibrils. Sulfuric acid acts by protonating glycosidic oxygen atoms, lowering the activation energy required for chain scission; however, once the concentration of soluble monosaccharides increases, the same acidic environment catalyzes dehydration reactions leading to furfural and HMF. Consequently, the optimum region corresponds to the point where the rate of polysaccharide hydrolysis exceeds the rate of sugar degradation, explaining the pronounced curvature observed in the response surface. Similar kinetic behavior has been described for dilute-acid hydrolysis optimized by response surface methodology, where maximum sugar recovery is obtained only within a limited severity window (Demirel *et al*., 2022; B. Zhang *et al*., 2022).

The temperature-RSL surface (Figure 6b) demonstrates that thermal severity alone is insufficient to maximize biomass conversion because hydrolysis efficiency also depends on catalyst transport through the lignocellulosic matrix. At lower RSL values (greater liquid availability), acid penetrates more uniformly into plant tissues, facilitating hemicellulose hydrolysis and increasing exposure of the amorphous cellulose fraction. As biomass loading increases, liquid accessibility decreases, generating internal diffusion limitations that reduce proton availability at reactive sites despite elevated temperatures. Therefore, sugar release becomes simultaneously controlled by intrinsic reaction kinetics and mass-transfer resistance, producing the broad valley observed in the response surface. Recent kinetic modeling studies similarly conclude that liquid-to-solid ratio significantly affects xylose recovery because diffusion limitations become increasingly important under high-solids operation (Velázquez-Herrera *et al*., 2024).

The acid-RSL surface (Figure 6c) presents a smoother curvature, indicating that sulfuric acid concentration and RSL mainly regulate catalyst utilization rather than reaction rate. Increasing acid concentration raises proton availability; nevertheless, its catalytic effectiveness depends on homogeneous distribution throughout the biomass particles. Under high biomass loading, limited liquid penetration reduces effective contact between the catalyst and structural carbohydrates, limiting hydrolysis efficiency even when acid concentration increases. This behavior indicates that catalyst accessibility becomes the limiting step before intrinsic acid strength, reinforcing that dilute-acid pretreatment is governed by the coupling of chemical catalysis and transport phenomena instead of catalyst concentration alone. Similar conclusions have been reported for sulfuric-acid hydrolysis of herbaceous lignocellulosic feedstocks, where reactor hydrodynamics and catalyst accessibility largely determine fermentable sugar recovery (Amarasekara & Nwankwo, 2023; Lv *et al*., 2024).

The nonlinear effects of temperature and sulfuric acid concentration may reflect the combined influence of polysaccharide hydrolysis and possible secondary reactions involving soluble carbohydrates. Under acid-catalyzed conditions, pentoses can undergo dehydration to form furfural

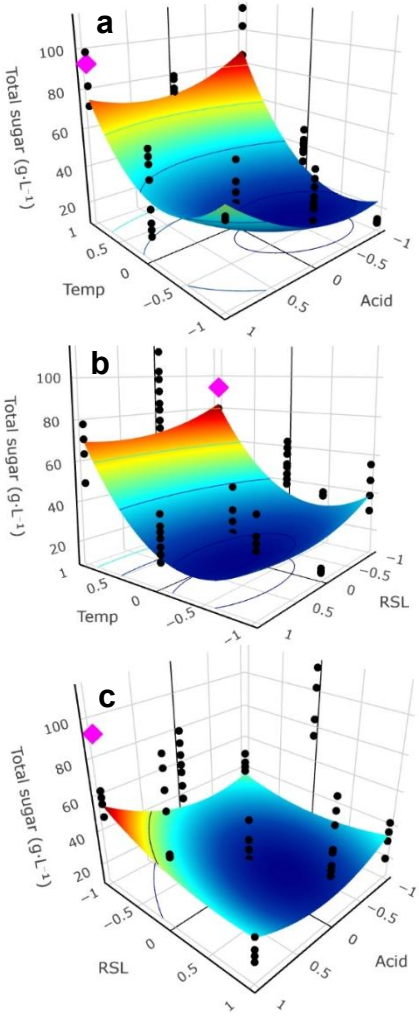


Fig. 6 Response surface plots: the combined effects of a) temperature-sulfuric acid concentration, b) temperature-RSL, and c) sulfuric acid concentration-RSL of *E. crassipes*

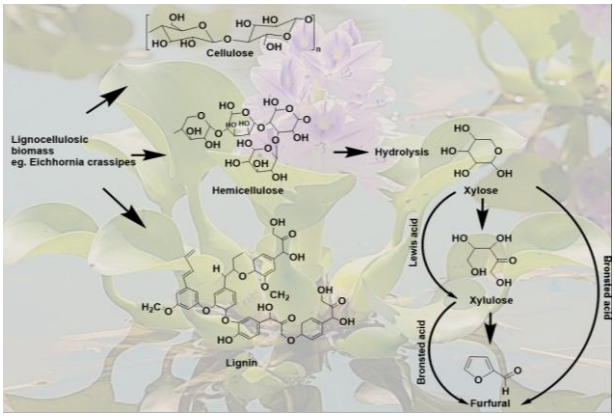


Fig. 8 Hydrolysis and dehydration of lignocellulosic biomass to furfural

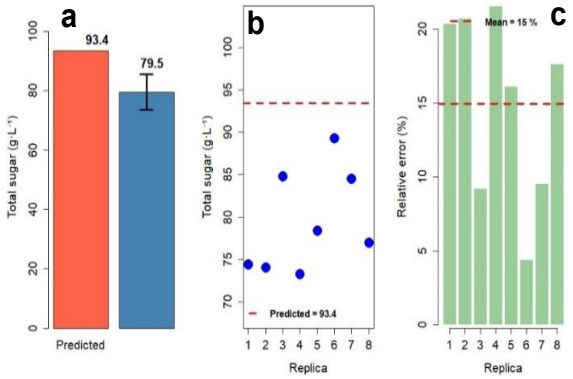


Fig. 7 Experimental validation of the BBD model for total sugar production during dilute-acid hydrolysis of *E. crassipes*: a) model validation, b) experimental replicates, and c) prediction error

(Figure 7), whereas hexoses can be converted into HMF through related dehydration pathways (Bakili *et al.*, 2025; Delbecq *et al.*, 2018; Wang *et al.*, 2025). However, these compounds were not quantified in the present study. Consequently, their formation cannot be confirmed from the total carbohydrate measurements, and the observed response surface cannot establish whether sugar degradation contributed to the decrease or nonlinear variation in the measured response. The effects identified by the Box–Behnken model should therefore be interpreted as statistical relationships between the operating conditions and the measured total carbohydrate concentration, while carbohydrate degradation remains a plausible, but unverified, chemical explanation.

$$TSc = 20.4 + 21.0T + 4.2A - 5.7RSL + 27.8T^2 + 12.6A^2 + 6.9RSL^2 - 11.1TA - 0.8TRSL - 4.8ARSL \quad (6)$$

where T is temperature; A is the acid concentration, and RSL is the solid-liquid relation.

The quadratic model provides mechanistic insight into the dilute-acid hydrolysis of *E. crassipes*, where each regression coefficient represents a specific physicochemical phenomenon involved in biomass deconstruction. 21.0T represents the effective thermal activation of the process. Increasing temperature supplies the energy required to overcome the recalcitrance of the lignocellulosic matrix, accelerating cleavage of glycosidic linkages and increasing carbohydrate accessibility. 4.2A represents the availability of catalytic protons (H^+). Sulfuric acid promotes protonation of glycosidic oxygen atoms, facilitating acid-catalyzed depolymerization of structural polysaccharides. The lower magnitude relative to temperature indicates that acid acts primarily as a catalyst rather than the main driving force (Du Pasquier *et al.*, 2023). −5.7RSL represents diffusion and mass-transfer limitations. Increasing solids loading decreases liquid accessibility and proton penetration into plant tissues, reducing catalyst effectiveness and limiting sugar release (Sun *et al.*, 2023). $27.8T^2$ indicates the existence of a thermal severity threshold. Once a critical temperature is reached, structural disruption of lignocellulose accelerates, producing the nonlinear increase described by the response surface. $12.6A^2$ represents the nonlinear catalytic response of sulfuric acid. Beyond a minimum proton concentration, hydrolysis efficiency increases rapidly until competitive degradation reactions progressively reduce process selectivity (Du Pasquier *et al.*, 2023). $6.9RSL^2$ indicates that transport phenomena become progressively more relevant as biomass loading increases, reflecting the nonlinear development of internal diffusion resistance. −11.1TA represents the competition between polysaccharide hydrolysis and sugar degradation. Simultaneously increasing temperature and acidity accelerates sugar formation but also promotes dehydration to furfural and HMF, defining the optimum hydrolysis severity. −0.8TRSL indicates that thermal energy cannot completely compensate for transport limitations, showing that heat transfer and catalyst diffusion remain coupled during hydrolysis. −4.8ARSL demonstrates that catalyst efficiency depends on accessibility rather than acid concentration alone. At higher solids loading, proton diffusion becomes restricted, reducing the effective catalytic action of sulfuric acid.

The experimental validation (Figure 8) showed that the quadratic model overestimated the optimum sugar concentration, predicting 93.4 g·L^{-1}, whereas the experimental validation yielded 79.5 ± 6.3 g·L^{-1}, corresponding to an average relative error of approximately 15%. This deviation indicates that the optimum lies within a region of pronounced surface curvature, where the strong interaction between temperature and acid concentration causes the quadratic polynomial to overestimate the maximum response. Similar behavior has been reported in lignocellulosic hydrolysis, where empirical RSM models accurately identify the optimum region but tend to overpredict responses under highly nonlinear reaction conditions. The experimental replicates indicate that the prediction error was not caused by a single outlier but was consistently distributed among all repetitions, suggesting that the deviation mainly originated from process variability rather than analytical uncertainty. This behavior can be attributed to the intrinsic heterogeneity of *E. crassipes*, including differences in cellulose and hemicellulose distribution, particle-size heterogeneity after milling, and local limitations in acid penetration through the lignocellulosic matrix. Additionally, incomplete removal of soluble compounds during biomass washing may promote secondary degradation reactions, contributing to lower experimental sugar recoveries than those predicted by the model.

The structural carbohydrate composition adopted for the mass balance (31% cellulose and 29% hemicellulose, dry basis) was established from recent experimental studies on whole *E. crassipes* biomass, which consistently reported cellulose contents between 30 and 32% and hemicellulose contents between 27 and 33% (Carreño-Sayago & Rodríguez-Parra, 2019; Lourenço *et al.*, 2026; Sayago *et al.*, 2024; Vázquez-Mendoza *et al.*, 2025).

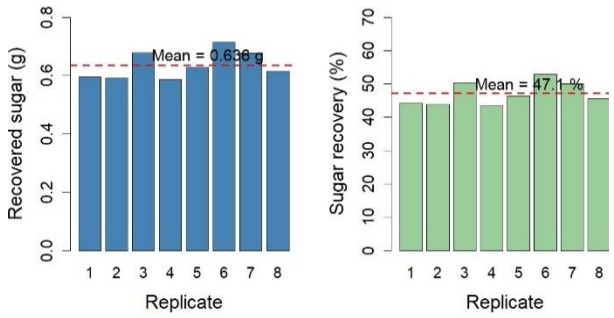


Fig. 9 Recovery of fermentable sugars under the optimized hydrolysis conditions

To complement the study, a simplified mass balance was performed under the optimum hydrolysis conditions predicted by the Box–Behnken model. The calculation was based on the eight validation experiments using 2 g of dry water hyacinth biomass and 10 mL of dilute sulfuric acid solution, from which approximately 8 mL of liquid hydrolysate was recovered after filtration. The amount of soluble sugars recovered was calculated by multiplying the measured TSc by the volume of recovered hydrolysate. The theoretical sugar potential was estimated from the structural carbohydrate content of water hyacinth, assuming 31% cellulose and 29% hemicellulose, together with the stoichiometric conversion factors of 1.11 for cellulose-to-glucose and 1.14 for hemicellulose-to-xylose conversion. Finally, sugar recovery efficiency was calculated as the ratio between the experimentally recovered sugars and the theoretical sugar potential.

Figure 9 demonstrates that the optimal conditions predicted by the model allow for highly reproducible sugar recovery. The mass-balance analysis estimated of soluble sugars recovered to range from 0.58 to 0.71 g, with an average of 0.636 g, equivalent to a mean recovery of 47.1% of the theoretical structural carbohydrate potential. Because the cellulose and hemicellulose contents were not experimentally determined for the specific biomass batch used in this study, this percentage should be interpreted as an estimated recovery relative to the assumed literature-based composition rather than as a direct measurement of the fraction of structural carbohydrates converted in the analyzed *E. crassipes* biomass. The reduced dispersion between replicates confirms that acid hydrolysis under the optimized conditions was stable and consistent, indicating that the variability observed during optimization was minimized.

4. Conclusions

The dilute sulfuric acid hydrolysis of *E.crassipes* was successfully optimized using a Box–Behnken experimental design, demonstrating that temperature is the dominant variable governing sugar release, while acid concentration and the RSL regulate catalytic selectivity and mass-transfer limitations. The statistical analysis confirmed the adequacy of the quadratic model (R^2 = 0.81), whereas the mechanistic interpretation of the regression coefficients revealed that sugar production results from the balance between polysaccharide depolymerization and the simultaneous degradation of released monosaccharides under increasing hydrolysis severity. Experimental validation showed good reproducibility of the optimized conditions despite the intrinsic heterogeneity of the biomass, indicating that most of the remaining prediction error originated from the structural variability of water hyacinth rather than from analytical uncertainty. Furthermore, the mass balance demonstrated an average recovery of 0.636 g of soluble sugars, corresponding to 47.1% of the theoretical structural carbohydrate potential, confirming that nearly half of the cellulose and hemicellulose available in the biomass was converted into soluble fermentable sugars under the selected operating conditions.

An important analytical limitation of this study is that the phenol–sulfuric acid assay provides an estimate of total carbohydrate concentration but does not distinguish individual monosaccharides or quantify furfural and HMF. Accordingly, the measured soluble sugar recovery cannot be used to establish the extent of sugar degradation or to determine the formation of these inhibitors. Future studies should combine total carbohydrate analysis with chromatographic quantification of individual sugars and degradation products to establish a more complete carbohydrate mass balance.

Acknowledgments

The authors acknowledge the Tecnológico Nacional de México/Instituto Tecnológico Superior de Coatzacoalcos (ITESCO), Veracruz, México, for the support and for providing space for this research. We also thank Rigoberto Ayala for his support in developing this study.

Author Contributions: D.M.: Conceptualization, formal analysis, supervision, writing—original draft. B.A.A.: methodology, formal analysis. J.A.C.V.: methodology. I.I.Z.R.: formal analysis. P.E.A.M. methodology. J.M.P.F.: formal analysis. R.S.G.P.: writing—review and editing. All authors have read and agreed to the published version of the manuscript.

Conflicts of Interest: The authors declare no conflict of interest.

References

Abba, A., Sabarinath, S., & Mustapha, R. A. (2025). Advancing circular bioeconomy through systematic review of multi-product biorefinery approaches for water hyacinth based renewable energy. *iScience*, *28*(7), 112807. https://doi.org/10.1016/j.isci.2025.112807

Adeyeni, S. A., Adewole, H. A., Lawal, B. M., Ogundepo, G. E., Obuotor, E. M., Olaleye, V. F., Adeoye, A. E., & Odufuwa, P. T. (2022). Growth performance and activities of some liver enzymes in Clarias gariepinus Burchell 1822 juveniles cultured in a water hyacinth (Eichhornia crassipes [Mart] Solms-Laubach) infested media. *Scientific African*, *18*, e01415. https://doi.org/10.1016/j.sciaf.2022.e01415

Amarasekara, A. S., & Nwankwo, V. C. (2023). A Comparison of Dilute Aqueous Isethionic Acid and Sulfuric Acid in Hydrolysis of Three Different Untreated Lignocellulosic Biomass Varieties. *Industrial & Engineering Chemistry Research*, *62*(46), 20037-20043. https://doi.org/10.1021/acs.iecr.3c02314

Aragaw, S. A., Yemata, T. A., Ayalew, A. A., Tadesse, A. A., Fekad, A. Y., Shibesh, A. K., Getie, F. A., Tessema, T. D., & Wubieneh, T. A. (2025). Improvement of bioethanol production from water hyacinth biomass by optimization of fermentation process conditions using response surface methodology. *Discover Applied Sciences*, *7*(4), 266. https://doi.org/10.1007/s42452-025-06635-9

Ashokkumar, V., Venkatkarthick, R., Jayashree, S., Chuetor, S., Dharmaraj, S., Kumar, G., Chen, W.-H., & Ngamcharussrivichai, C. (2022). Recent advances in lignocellulosic biomass for biofuels and value-added bioproducts—A critical review. *Bioresource Technology*, *344*, 126195. https://doi.org/10.1016/j.biortech.2021.126195

Atilago, A., Sadio Sidibé, S. D., Sossou, S. K., Nabulime, M. N., McCoy, E. L., Sawadogo, M., & Lansing, S. (2025). Enhancing bioenergy

from water hyacinth: Pretreatment and anaerobic co-digestion. *Bioresource Technology*, *437*, 133070. https://doi.org/10.1016/j.biortech.2025.133070

Babisk, M. P., Sales Barreto, G. N., Bornili Gadioli, M. C., Girondi Delaqua, G. C., Monteiro, S. N., & Fontes Vieira, C. M. (2023). Incorporation of Eichhornia crassipes dry biomass in red ceramics aiming at energy savings during the firing stage. *Journal of Materials Research and Technology*, *25*, 522-531. https://doi.org/10.1016/j.jmrt.2023.05.052

Bajpai, S., & Nemade, P. R. (2023). An integrated biorefinery approach for the valorization of water hyacinth towards circular bioeconomy: A review. *Environmental Science and Pollution Research*, *30*(14), 39494-39536. https://doi.org/10.1007/s11356-023-25830-y

Bakili, S., Kivevele, T., Kichonge, B., Salifu, A. A., & King'ondu, C. K. (2025). Furfural from lignocellulose biomass a comprehensive review of hydrolysis methods production technologies and integration into the circular economy. *Discover Sustainability*, *6*(1), 870. https://doi.org/10.1007/s43621-025-01644-5

Basaula, R., Sharma, H. P., Paudel, B. R., Kunwar, P. S., & Sapkota, K. (2023). Effects of invasive water hyacinth on fish diversity and abundance in the Lake Cluster of Pokhara Valley, Nepal. *Global Ecology and Conservation*, *46*, e02565. https://doi.org/10.1016/j.gecco.2023.e02565

Carreño-Sayago, U. F., & Rodríguez-Parra, C. (2019). Eichhornia crassipes (Mart.) Solms: Un sistema integral de fitorremediación y bioenergía. *Revista Chapingo Serie Ciencias Forestales y del Ambiente*, *25*(3), 399-411. https://doi.org/10.5154/r.rchscfa.2018.06.051

Chinwatpaiboon, P., Savarajara, A., & Luengnaruemitchai, A. (2023). Enzymatic hydrolysate of water hyacinth with NaOH pretreatment for biobutanol production via ABE fermentation by Clostridium beijerinckii JCM 8026. *Biomass and Bioenergy*, *173*, 106782. https://doi.org/10.1016/j.biombioe.2023.106782

Damtie, Y. A., Mengistu, D. A., & Meshesha, D. T. (2021). Spatial coverage of water hyacinth (Eichhornia crassipes (Mart.) Solms) on Lake Tana and associated water loss. *Heliyon*, *7*(10), e08196. https://doi.org/10.1016/j.heliyon.2021.e08196

Das, S., Bhattacharya, A., Haldar, S., Ganguly, A., Gu, S., Ting, Y. P., & Chatterjee, P. K. (2015). Optimization of enzymatic saccharification of water hyacinth biomass for bio-ethanol: Comparison between artificial neural network and response surface methodology. *Sustainable Materials and Technologies*, *3*, 17-28. https://doi.org/10.1016/j.susmat.2015.01.001

Delbecq, F., Wang, Y., Muralidhara, A., El Ouardi, K., Marlair, G., & Len, C. (2018). Hydrolysis of Hemicellulose and Derivatives—A Review of Recent Advances in the Production of Furfural. *Frontiers in Chemistry*, *6*, 146. https://doi.org/10.3389/fchem.2018.00146

Demirel, F., Germec, M., & Turhan, I. (2022). Fermentable sugars production from wheat bran and rye bran: Response surface model optimization of dilute sulfuric acid hydrolysis. *Environmental Technology*, *43*(24), 3779-3800. https://doi.org/10.1080/09593330.2021.1934563

Deng, H.-Q., Lin, X.-H., Fan, J.-T., Fu, P.-Z., Guan, J.-J., Lei, H.-L., Liu, L.-H., Lai, L.-H., Hou, X.-D., & Lou, W.-Y. (2023). Glycolic acid-based deep eutectic solvents boosting co-production of xylo-oligomers and fermentable sugars from corncob and the related kinetic mechanism. *Biotechnology for Biofuels and Bioproducts*, *16*(1), 126. https://doi.org/10.1186/s13068-023-02369-1

Ding, K., Liu, D., Chen, X., Zhang, H., Shi, S., Guo, X., Zhou, L., Han, L., & Xiao, W. (2024). Scalable lignocellulosic biorefineries: Technoeconomic review for efficient fermentable sugars production. *Renewable and Sustainable Energy Reviews*, *202*, 114692. https://doi.org/10.1016/j.rser.2024.114692

Djihouessi, M. B., Olokotum, M., Chabi, L. C., Mouftaou, F., & Aina, M. P. (2023). Paradigm shifts for sustainable management of water hyacinth in tropical ecosystems: A review and overview of current challenges. *Environmental Challenges*, *11*, 100705. https://doi.org/10.1016/j.envc.2023.100705

Du Pasquier, J., Paës, G., & Perré, P. (2023). Principal factors affecting the yield of dilute acid pretreatment of lignocellulosic biomass: A critical review. *Bioresource Technology*, *369*, 128439. https://doi.org/10.1016/j.biortech.2022.128439

Dubois, Michel., Gilles, K. A., Hamilton, J. K., Rebers, P. A., & Smith, Fred. (1956). Colorimetric Method for Determination of Sugars and Related Substances. *Analytical Chemistry*, *28*(3), 350-356. https://doi.org/10.1021/ac60111a017

Elma, M., Kadek Devi Ananda Saraswati, N., Fransiska Afrida Simatupang, P., Febriyanti, R., Rahma, A., & Ria Mustalifah, F. (2023). Hydrogel derived from water hyacinth and pectin from banana peel as a membrane layer. *Materials Today: Proceedings*, *87*, 13-17. https://doi.org/10.1016/j.matpr.2023.01.368

Godana, G., Fufa, F., & Debesa, G. (2022). Eichhornia crassipes expansion detection using geospatial techniques: Lake Dambal, Oromia, Ethiopia. *Environmental Challenges*, *9*, 100616. https://doi.org/10.1016/j.envc.2022.100616

Ingabire, H., Twizerimana, M., & M. M'Arimi, M. (2023). Effect of co-digestion with water hyacinth, inoculum concentration and dilution on biogas production of fish waste. *Energy Reports*, *9*, 286. https://doi.org/10.1016/j.egyr.2023.05.072

Lourenço, A., Gomes, T., Bernardo, M., Matos, I., Lapa, N., & Gominho, J. (2026). Valorization of Water Hyacinth Biomass: Comprehensive Characterization and Production and Application of Activated Carbons. *BioEnergy Research*, *19*(1), 46. https://doi.org/10.1007/s12155-026-10967-8

Lv, Y., Zhang, Y., & Xu, Y. (2024). Understanding and technological approach of acid hydrolysis processing for lignocellulose biorefinery: Panorama and perspectives. *Biomass and Bioenergy*, *183*, 107133. https://doi.org/10.1016/j.biombioe.2024.107133

McNamara, C., O'Shea, A., Rao, P., Ure, A., Ayarde-Henríquez, L., Ghaani, M. R., Ross, A., & Dooley, S. (2024). Steady states and kinetic modelling of the acid-catalysed ethanolysis of glucose, cellulose, and corn cob to ethyl levulinate. *Energy Advances*, *3*(6), 1439-1458. https://doi.org/10.1039/D4YA00043A

Mishima, D., Kuniki, M., Sei, K., Soda, S., Ike, M., & Fujita, M. (2008). Ethanol production from candidate energy crops: Water hyacinth (Eichhornia crassipes) and water lettuce (Pistia stratiotes L.). *Bioresource Technology*, *99*(7), 2495-2500. https://doi.org/10.1016/j.biortech.2007.04.056

Phan, Q. H. H., Le, H. Q. A., & Nguyen, P. K. T. (2025). Biohydrogen production from water hyacinth–A review of pretreatment, production, and purification processes. *Biomass and Bioenergy*, *201*, 108078. https://doi.org/10.1016/j.biombioe.2025.108078

Rezania, S., Md Din, M. F., Eva Mohamad, S., Sohaili, J., Mat Taib, S., Mohd Yusof, M. B., Kamyab, H., Darajeh, N., & Ahsan, A. (2017). Review on pretreatment methods and ethanol production from cellulosic water hyacinth. *BioResources*, *12*(1), 2108-2124. https://doi.org/10.15376/biores.12.1.Rezania

Romero-Borbón, E., Oropeza-González, A. E., González-García, Y., & Córdova, J. (2022). Thermochemical and Enzymatic Saccharification of Water Hyacinth Biomass into Fermentable Sugars. *Processes*, *10*(2), 210. https://doi.org/10.3390/pr10020210

Sayago, U. F. C., Gómez-Caicedo, M. I., & Mercado Suárez, Á. L. (2024). Design of a sustainable system for wastewater treatment and generation of biofuels based on the biomass of the aquatic plant Eichhornia Crassipes. *Scientific Reports*, *14*(1), 11068. https://doi.org/10.1038/s41598-024-61239-4

Sierra, C. G., Wong Arguelles, C., Hernández Orduña, M. G., & Murrieta Galindo, R. (2024). Caracterización de la composición química de Pontederia crassipes de la laguna de Casa Blanca y el río Coatzacoalcos en el estado de Veracruz (Mexico). *Revista Brasileira de Meio Ambiente*, *12*(2). https://doi.org/10.66205/rvbma.v12i2.1673

Singh, J. K., Chaurasia, B., Dubey, A., Faneite Noguera, A. M., Gupta, A., Kothari, R., Upadhyaya, C. P., Kumar, A., Hashem, A., Alqarawi, A. A., & Abd Allah, E. F. (2020). Biological Characterization and Instrumental Analytical Comparison of Two Biorefining Pretreatments for Water Hyacinth (Eichhornia crassipes) Biomass Hydrolysis. *Sustainability*, *13*(1), 245. https://doi.org/10.3390/su13010245

Sun, C., Meng, X., Sun, F., Zhang, J., Tu, M., Chang, J.-S., Reungsang, A., Xia, A., & Ragauskas, A. J. (2023). Advances and perspectives on mass transfer and enzymatic hydrolysis in the enzyme-mediated lignocellulosic biorefinery: A review. *Biotechnology Advances*, *62*, 108059. https://doi.org/10.1016/j.biotechadv.2022.108059

Świątek, K., Gaag, S., Klier, A., Kruse, A., Sauer, J., & Steinbach, D. (2020). Acid Hydrolysis of Lignocellulosic Biomass: Sugars and Furfurals Formation. *Catalysts*, *10*(4), 437. https://doi.org/10.3390/catal10040437

Tovar-Jiménez, X., Favela-Torres, E., Volke-Sepúlveda, T. L., Escalante-Espinosa, E., Díaz-Ramírez, I. J., Córdova-López, J. A., & Téllez-Jurado, A. (2019). Influence of the geographical area and morphological part of the water hyacinth on its chemical composition. *Ingeniería Agrícola y Biosistemas*, *11*(1). https://doi.org/10.5154/r.inagbi.2017.10.013

Tucker, C. S., & Debusk, T. A. (1981). Seasonal growth of Eichhornia crassipes (Mart.) solms: Relationship to protein, fiber, and available carbohydrate content. *Aquatic Botany*, *11*, 137-141. https://doi.org/10.1016/0304-3770(81)90055-3

Udume, O. A., Abu, G. O., Stanley, H. O., Vincent-Akpu, I. F., & Momoh, Y. (2022). Impact of composting factors on the biodegradation of lignin in Eichhornia crassipes (water hyacinth): A response surface methodological (RSM) investigation. *Heliyon*, *8*(9), e10340. https://doi.org/10.1016/j.heliyon.2022.e10340

Vázquez-Mendoza, C., Leyva-Ramos, R., Medellín-Castillo, N. A., Carrales-Alvarado, D. H., & Aragón-Piña, A. (2025). CADMIUM(II) removal from aqueous solution by adsorption on water hyacinth (Eichhornia crassipes) hydrochar modified with citric acid. *Case Studies in Chemical and Environmental Engineering*, *12*, 101267. https://doi.org/10.1016/j.cscee.2025.101267

Velázquez-Herrera, L. A., Cobos-Murcia, J. Á., Bolaños-Reynoso, E., & López-Zamora, L. (2024). Modelling and dynamic simulation to produce fermentable sugars from lignocellulosic substrates through dilute acid hydrolysis. *The Canadian Journal of Chemical Engineering*, *102*(8), 2739-2753. https://doi.org/10.1002/cjce.25223

Velvizhi, G., Balakumar, K., Shetti, N. P., Ahmad, E., Kishore Pant, K., & Aminabhavi, T. M. (2022). Integrated biorefinery processes for conversion of lignocellulosic biomass to value added materials: Paving a path towards circular economy. *Bioresource Technology*, *343*, 126151. https://doi.org/10.1016/j.biortech.2021.126151

Wang, Y., Li, M., Wang, Z., Liu, S., & O'Young, L. (2025). Furfural production: A review on reaction mechanism and conventional production process. *Industrial Crops and Products*, *230*, 121103. https://doi.org/10.1016/j.indcrop.2025.121103

Yuan, Q., Liu, S., Ma, M.-G., Ji, X.-X., Choi, S.-E., & Si, C. (2021). The Kinetics Studies on Hydrolysis of Hemicellulose. *Frontiers in Chemistry*, *9*, 781291. https://doi.org/10.3389/fchem.2021.781291

Zhang, B., Wu, L., Wang, Y., Li, J., Zhan, B., & Bao, J. (2022). Re-examination of dilute acid hydrolysis of lignocellulose for production of cellulosic ethanol after de-bottlenecking the inhibitor barrier. *Journal of Biotechnology*, *353*, 36-43. https://doi.org/10.1016/j.jbiotec.2022.05.006

Zhang, J., Wang, Y., Du, X., & Qu, Y. (2020). Selective removal of lignin to enhance the process of preparing fermentable sugars and platform chemicals from lignocellulosic biomass. *Bioresource Technology*, *303*, 122846. https://doi.org/10.1016/j.biortech.2020.122846

Zhang, Q., Wei, Y., Han, H., & Weng, C. (2018). Enhancing bioethanol production from water hyacinth by new combined pretreatment methods. *Bioresource Technology*, *251*, 358-363. https://doi.org/10.1016/j.biortech.2017.12.085

Zhou, Z., Liu, D., & Zhao, X. (2021). Conversion of lignocellulose to biofuels and chemicals via sugar platform: An updated review on chemistry and mechanisms of acid hydrolysis of lignocellulose. *Renewable and Sustainable Energy Reviews*, *146*, 111169. https://doi.org/10.1016/j.rser.2021.111169

© 2027. The Author(s). This article is an open access article distributed under the terms and conditions of the Creative Commons Attribution-ShareAlike 4.0 (CC BY-SA) International License (http://creativecommons.org/licenses/by-sa/4.0/)